Research Paper

Microbiome Remodeling *via* the Montmorillonite Adsorption-Excretion Axis Prevents Obesity-related Metabolic Disorders

Pengfei Xu [a], Fan Hong [a], Jialin Wang [a], Yusheng Cong [c], Shu Dai [a], Sheng Wang [a], Jing Wang [d], Xi Jin [a,b], Fang Wang [e], Jin Liu [a,b], Yonggong Zhai [a,b,*]

[a] *Beijing Key Laboratory of Gene Resource and Molecular Development, College of Life Sciences, Beijing Normal University, Beijing 100875, China*
[b] *Key Laboratory for Cell Proliferation and Regulation Biology of State Education Ministry, College of Life Sciences, Beijing Normal University, Beijing 100875, China*
[c] *Institute of Aging Research, School of Medicine, Hangzhou Normal University, Hangzhou 311121, China*
[d] *Department of Biology Science and Technology, Baotou Teacher's College, Baotou 014030, China*
[e] *Department of Medical Genetics and Cell Biology, School of Basic Sciences, Guangzhou Medical University, Guangzhou 511436, China*

ARTICLE INFO

ABSTRACT

Obesity and its related metabolic disorders are closely correlated with gut dysbiosis. Montmorillonite is a common medicine used to treat diarrhea. We have previously found that dietary lipid adsorbent-montmorillonite (DLA-M) has an unexpected role in preventing obesity. The aim of this study was to further investigate whether DLA-M regulates intestinal absorption and gut microbiota to prevent obesity-related metabolic disorders. Here, we show that DLA-M absorbs free fatty acids (FFA) and endotoxins *in vitro* and *in vivo*. Moreover, the combination of fluorescent tracer technique and polarized light microscopy showed that DLA-M crystals immobilized BODIPY® FL C16 and FITC-LPS, respectively, in the digestive tract *in situ*. HFD-fed mice treated with DLA-M showed mild changes in the composition of the gut microbiota, particularly increases in short-chain fatty acids (SCFA)-producing *Blautia* bacteria and decreases in endotoxin-producing *Desulfovibrio* bacteria, these changes were positively correlated with obesity and inflammation. Our results indicated that DLA-M immobilizes FFA and endotoxins in the digestive tract *via* the adsorption-excretion axis and DLA-M may potentially be used as a prebiotic to prevent intestinal dysbiosis and obesity-associated metabolic disorders in obese individuals.

© 2017 The Authors. Published by Elsevier B.V. This is an open access article under the CC BY-NC-ND license (http://creativecommons.org/licenses/by-nc-nd/4.0/).

1. Introduction

Obesity is a metabolic disturbance that has high prevalence worldwide and has increased over the past four decades. It is associated with several chronic diseases, including type 2 diabetes (T2D), nonalcoholic fatty liver disease (NAFLD), dyslipidemia, cardiovascular diseases and cancer, which are the main causes of mortality (Wormser et al., 2011, Bhaskaran et al., 2014, Arnold et al., 2015). Obesity results from a complex interaction between genetic background and environmental factors, such

as a fatty diet and low physical activity (Everard and Cani, 2013). When fat synthesis continually exceeds lipolysis, the surplus lipids are stored in white adipose tissue (WAT), thus leading to the development of obesity (Hoffmann et al., 2015). The overweight and obesity epidemic poses a considerable global public health threat. The treatment and prevention of obesity and its complications are a major challenge at present.

The connection between the intestinal microbiota and energy homeostasis and the pathogenesis of obesity-associated metabolic disorders is increasingly being recognized (Musso et al., 2010, Hildebrandt et al., 2009). Accumulating evidence suggests that changes in the gut microbiota composition are associated with glucose metabolism, lipid metabolism, energy balance and immune homeostasis, thereby influencing whole-body metabolism (Cani, 2014). Approximately 1000 different bacterial species exist in the human gut, and these bacteria have 150 times more genes than humans do (Qin et al., 2010). Hosts and their gut microbiomes have co-evolved, and the gut microbiome thus regulates the host metabolism and extraction of energy from ingested food (Shen et al., 2013, Shin et al., 2014). The intestinal microbiota exchange metabolites with the host and perform a crosstalk with host signaling pathways, thereby modulating both host gene expression and host metabolism.

Increasing clinical and experimental data indicate that bacteria lipopolysaccharide (LPS), or endotoxin, is closely related to the development of obesity-associated low-grade inflammation (Cani et al., 2008, 2009). High plasma endotoxemia may result from the increase in Gram-negative bacteria in the gut microbiota and intestinal permeability that result from a high fat diet (HFD) (Serino et al., 2012). Moreover, LPS treatment causes mild obesity and NAFLD in mice and humans (Chen et al., 2011, Thuy et al., 2008, Harte et al., 2010). These observations indicate that decreasing the amount of endotoxin in the bloodstream may protect animals against obesity induced inflammation.

We have previously shown that dietary lipid adsorbent-montmorillonite (DLA-M) can adsorb dietary lipids (triglycerides and cholesterol) and increase fecal lipid excretion, thus preventing obesity in HFD-fed rats (Xu et al., 2016). The adsorption-excretion axis decreases the energy intake from the digestive tract. In the present study, we further found that DLA-M also adsorbs free fatty acids (FFA) and endotoxin and affects the composition of the gut microbiota, thereby preventing obesity, improving insulin sensitivity and ameliorating hepatic steatosis in mouse model of obesity. Our results thus demonstrate that DLA-M is an excellent adsorbent agent that may potentially contribute to the prevention of obesity and its associated metabolic disorders.

2. Materials & Methods

2.1. Materials

DLA-M was prepared in our laboratory, as previously described (Xu et al., 2016). BODIPY (D3922) and BODIPY® FL C16 (D3821) were obtained from Thermo Fisher Scientific. Lipopolysaccharides (LPS), FITC-LPS (F3665), oleic acid (OA) and palmitic acid (PA) were purchased from Sigma-Aldrich.

2.2. Animal Experiments

Animal experiments were approved and performed in accordance with the guidelines of Ethics and Animal Welfare Committee of Beijing Normal University (Approval No. CLS-EAW-2013-014 and CLS-EAW-2015-013). C57BL/6J and CD-1 (ICR) mice were purchased from Vital River Laboratory Animal Technology Co. Ltd. (Beijing, China) and housed in a light and climate controlled room at 12 h light - dark cycle and 25 ± 2 °C, 3–4 mice/cage, with free access to water and different diets. Both the normal chow diet (NCD) and HFD (containing 60% and 45% fat by energy, as shown in Supplementary Table 1) were obtained from Beijing HFK Bioscience Co. Ltd. (China). Ten-week-old male C57BL/6J mice were randomly allocated into three groups containing six to fifteen animals each, and they were fed the NCD or HFD (60% kcal fat) for ten weeks. Ten-week-old male CD-1 mice were randomly distributed into three groups of 10 animals each, and they were fed NCD or HFD (45% kcal fat) for five weeks (Supplementary Figs. 1a–f and 2a–d). The treatment groups (HFD + DLA-M) were fed an HFD with DLA-M at 1 g/kg body weight by intragastric gavage daily, whereas the NCD and HFD groups, which were used as controls, were orally administered normal saline. The body weight and food intake were measured weekly. Fresh stool samples were collected during the final five days and immediately stored at −80 °C for further analysis. During the final two weeks of the experiment, six animals from each group were subjected to the oral glucose tolerance test (OGTT), introperitoneal glucose tolerance test (IGTT) and insulin tolerance test (ITT) according to previously described methods (Gao et al., 2009). At the end of the experimental period, all mice were starved for 12 h and then sacrificed. Blood was collected from the eye venous plexus. The epididymal-WAT (Epi-WAT), perirenal-WAT (Per-WAT), mesenteric-WAT (Mes-WAT), liver and gastrointestinal system (with or without chyme) were immediately excised, weighed, measured and frozen in liquid nitrogen after sacrifice.

Ten-week-old male RFP (Rosa26-mTmG) mice ($n = 3$) were treated with DLA-M (1 g/kg) and then treated with BODIPY® FL C16 (5 mg/kg) or FITC-LPS (5 mg/kg) separately by gavage for 4 h, and the mice were observed with a whole-body imaging scope (Lumazone FA1300, USA).

2.3. Cell Culture and Steatotic Hepatocyte Model Construction

L-02 cells were obtained from the Cell Resource Center, Peking Union Medical College (Beijing, China), and they were cultured in DMEM containing 10% FBS and 1% penicillin-streptomycin at 37 °C with 5% CO_2. Steatotic hepatocyte model construction was performed as previously described (Gomez-Lechon et al., 2007, Zhou et al., 2014). L-02 cells at 75% confluency were exposed to a 1 mmol/l FFA mixture (OA:PA ratio, 2:1). After incubation for another 48 h, the cells were used for further analysis.

2.4. Quantitative Real-time PCR

Total RNA was isolated using an RNAprep Pure tissue kit or RNAprep Pure cell kit (Tiangen, China). Equal amounts of total RNA (2 μg) were then reverse transcribed to cDNA using M-MLV transcriptase (Promega, USA). Quantitative real-time PCR was performed in triplicate using the SYBR Green qPCR SuperMix (Transgen Biotech, China) on an ABI 7500 instrument (Applied Biosystems, USA) according to the manufacturer's instructions. Gene expression was normalized against the housekeeping gene: murine or human glyceraldehyde-3-phosphate dehydrogenase (GAPDH). The primers used are listed in Supplementary Table 2.

2.5. Western Blot Analyses

An equal amount of cell or tissue protein lysates (10 μg) was subjected to 10% SDS-PAGE and electro-blotted onto Immobilon®-P transfer membranes (Millipore, USA). Then western blot analysis was performed using standard procedures. The band intensity was quantified using ImageJ software. The following antibodies were used: antibodies against FABP (sc-18661), TLR-4 (sc-293072), NF-κB (sc-372) and IκB-α (sc-847) from Santa Cruz, and antibodies against β-actin from Sigma.

2.6. Biochemical Analyses

ELISA kits were used to evaluate insulin, tumor necrosis factor α (TNFα), and interleukin-6 (IL-6), which were purchased from Neobioscience (China). Serum endotoxin and LPS content quantification were performed using a quantitative chromogenic tachypleus amebocyte lysate kit, which was purchased from the Chinese Horseshoe Crab Reagent Manufactory, Co., Ltd. Triglyceride (TG), total cholesterol (TC), and FFA concentrations in serum, tissue or cell were measured using commercially available kits from Applygen Technologies Inc. (China).

2.7. Histological Analyses

Tissues were fixed in 4% formaldehyde, embedded in paraffin, sectioned at 5 μm, and stained with hematoxylin and eosin. The sizes of the adipocytes and the proximal jejunum villi length were analyzed using Image-pro plus software. To observe the lipid droplets, frozen liver sections and steatotic L-02 cells were staining by using Oil Red O or BODIPY.

2.8. DLA-M Absorption Analyses

For the *in vivo* experiment, RFP mice were treated as described above, and the gastrointestinal contents (stomach, duodenum, jejunum, ileum, cecum and colon) were evaluated by using smears. BODIPY® FL C16 and FITC-LPS were visualized as green fluorescence at an absorbance wavelength of 488 nm using a fluorescence microscope (ZEISS Imager M1, Germany), and DLA-M crystals were detected using a polarized brightfield *in situ*. For the *in vitro* experiment, the intestinal chyme was diluted with saline or certain concentrations of OA, PA and LPS and then

treated with 0–400 mg/ml DLA-M, laumontite and maifanite for 6 h. Afterward, the supernatant concentration was measured.

2.9. Gut Microbiota Profiling

Bacterial DNA was extracted from fecal samples with a QIAamp DNA stool Mini Kit (Qiagen, Germany). PCR amplified with barcoded specific bacterial primers targeting the 16S rRNA gene V3–V4 regions, primer forward: 5′-ACTCCTACGGGA -GGCAGCA-3′, and reverse: 5′-GGACTACHVGGGTWTCTAAT-3′. Sequencing libraries were sequenced on an Illumina MiSeq platform at Biomarker Technologies Co, Ltd. (Beijing, China). The rawdata were merged using FLASH (Magoc and Salzberg, 2011). Sequences were quality filtered using Trimmomatic (Bolger et al., 2014), and Chimera sequences were identifically removed using the UCHIME algorithm (Edgar et al., 2011). The resulting sequences were then aligned against the Greengenes database of 16S rRNA gene sequences. The operational taxonomic unit (OUT) was delineated at a 97% similarity level with UCLUST (Edgar, 2010). Alpha diversity analysis, which included OTU-Venn, Shannon index and beta diversity analysis, which included UniFrac distance-based principal coordinates analysis (PCoA) and the Bray-Curtis cluster tree using the unweighted pair-group method with arithmetic mean (UPGMA) analysis

and heatmap were performed using QIIME (Caporaso et al., 2010). The LDA effect size (LEfSe) analysis (Segata et al., 2011) was used for the quantitative analysis of biomarkers within different groups.

2.10. Statistical Analyses

All values were obtained from at least three replicate experiments and are expressed as the mean $\pm$ s.e.m. Differences between groups were statistically analyzed using one-way ANOVA, which was followed by Tukey's multiple comparison tests and unpaired t-tests. LEfSe analysis first used the non-parametric factorial Kruskal-Wallis (KW) sum-rank test and then used the (unpaired) Wilcoxon rank-sum test. Data that did not meet the analysis of variance assumptions were analyzed with the Mann-Whitney test. Differences were considered statistically significant at $P < 0.05$.

3. Results

3.1. DLA-M Prevents HFD-induced Obesity and Insulin Resistance in Mice

Two mouse models of obesity 10-week-old male C57BL/6J and CD-1 mice were fed NCD or HFD for 10 and 5 weeks, respectively. In agreement
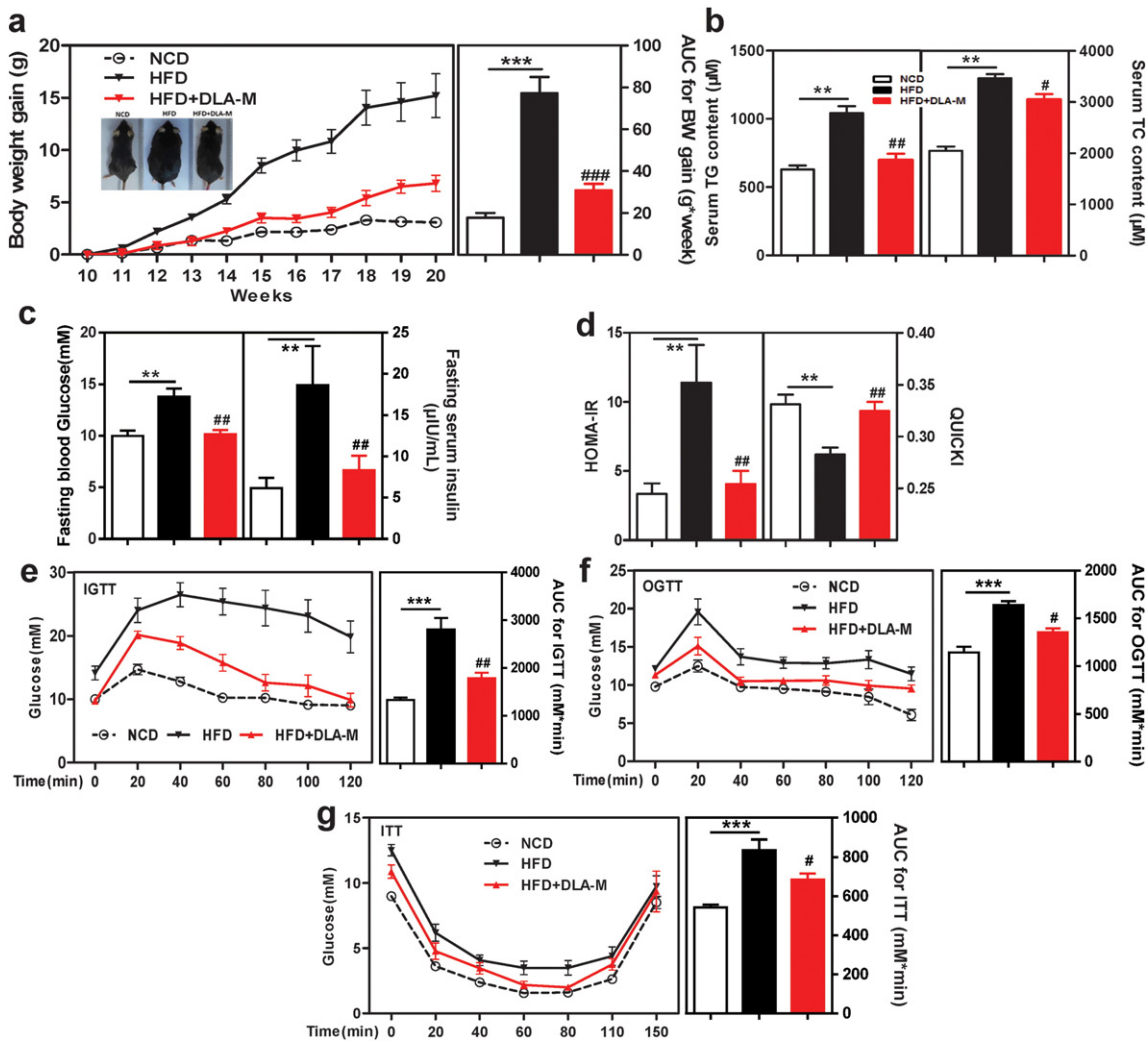
Fig. 1. DLA-M decreases body weight and improves insulin resistance in HFD C57BL/6J mice. NCD and HFD (60% kcal fat) C57BL/6J mice were treated daily with water or 1 g/kg/day DLA-M by intragastric gavage for 10 weeks ($n = 6$–15). Effects of DLA-M treatment on the body weight gain and the calculated AUC (a), serum TG and TC content (b), fasting blood glucose and serum insulin levels (c), and calculated HOMA-IR and QUICKI values (d) are shown. IGTT (e); OGTT (f); ITT (g) results. Curves of the blood glucose levels and the calculated AUC are shown. Values are expressed as the means $\pm$ s.e.m. **, $P < 0.01$; ***, $P < 0.001$ compared with NCD. #, $P < 0.05$; ##, $P < 0.01$; and ###, $P < 0.001$ compared with HFD. Differences were assessed by ANOVA with Tukey's multiple comparison test.

with previous work using an obese rat model (Xu et al., 2016), DLA-M prevented body weight gain in each animal model, but did not cause a significant change in the relative food intake of CD-1 mice (Fig. 1a and Supplementary Fig. 1a–c). Because obesity is strongly associated with insulin resistance, a typical characteristic of T2D, we measured the fasting blood glucose and insulin concentrations and calculated the homeostasis model index of insulin resistance (HOMA-IR: insulin ∗ glucose ⁄ 22.5) and the quantitative insulin check index of insulin sensitivity (QUICKI: 1 ⁄ [log(insulin) + log(glucose)]). DLA-M treatment significantly improved insulin sensitivity of the mice and reversed the two indexes to nearly normal levels (Fig. 1c and d), a result further confirmed by IGTT (Fig. 1e), OGTT (Fig. 1f) and ITT (Fig. 1g) analyses in C57BL/6J mice.

3.2. DLA-M Inhibits Fat Accumulation in Adipose Tissues and Ameliorates Hepatic Steatosis in HFD Mice

We isolated the following three types of WAT: Epi-WAT, Per-WAT and Mes-WAT. DLA-M treatment reduced the various ratios of WAT/BW by >40% compared with those in the C57BL/6J mice that were given an HFD without DLA-M (Fig. 2a–c). The slight effect of DLA-M on inhibition of fat accumulation in WAT was also evident in the CD-1 mouse model (Supplementary Fig. 1d and e). Next, we measured the sizes of adipocyte cells obtained from Epi-WAT sections by automated

imaging analysis (Fig. 2d). DLA-M in combination with the HFD, compared with the HFD alone, decreased the mean adipocyte size by 45.6% (Fig. 2e), thus reflecting the increased frequency of smaller adipocytes and the decreased frequency of larger adipocytes (Fig. 2f). The serum lipid concentrations (TG and TC) were lower in the HFD + DLA-M-treated group than in the HFD-fed group of C57BL/6J mice (Fig. 1b). A decrease in hyperlipidemia is associated with ameliorated hepatic steatosis. Oil Red O staining and the liver TG content analysis indicated that DLA-M effectively inhibited lipid infiltration in the mouse livers (Fig. 2g and h). The expression levels of fatty acid metabolism and lipogenic genes were decreased in the hepatic and adipose tissues of HFD mice after DLA-M treatment (Fig. 2i and Supplementary Fig. 2a–d). Furthermore, western blot analysis of liver fatty acid transport protein (FABP) was also performed in C57BL/6J mice (Fig. 2j). These results indicated that DLA-M prevents HFD-induced obesity-related metabolic syndrome.

3.3. DLA-M Inhibits Lipogenesis via Immobilizing FFA in the Digestive Tract

The concentration of circulating FFA, also known as non-esterified fatty acids (NEFA), is strongly associated with several adverse metabolic effects, especially insulin resistance and T2D (Karpe et al., 2011, Arner and Ryden, 2015). We then investigated the fasting circulating NEFA
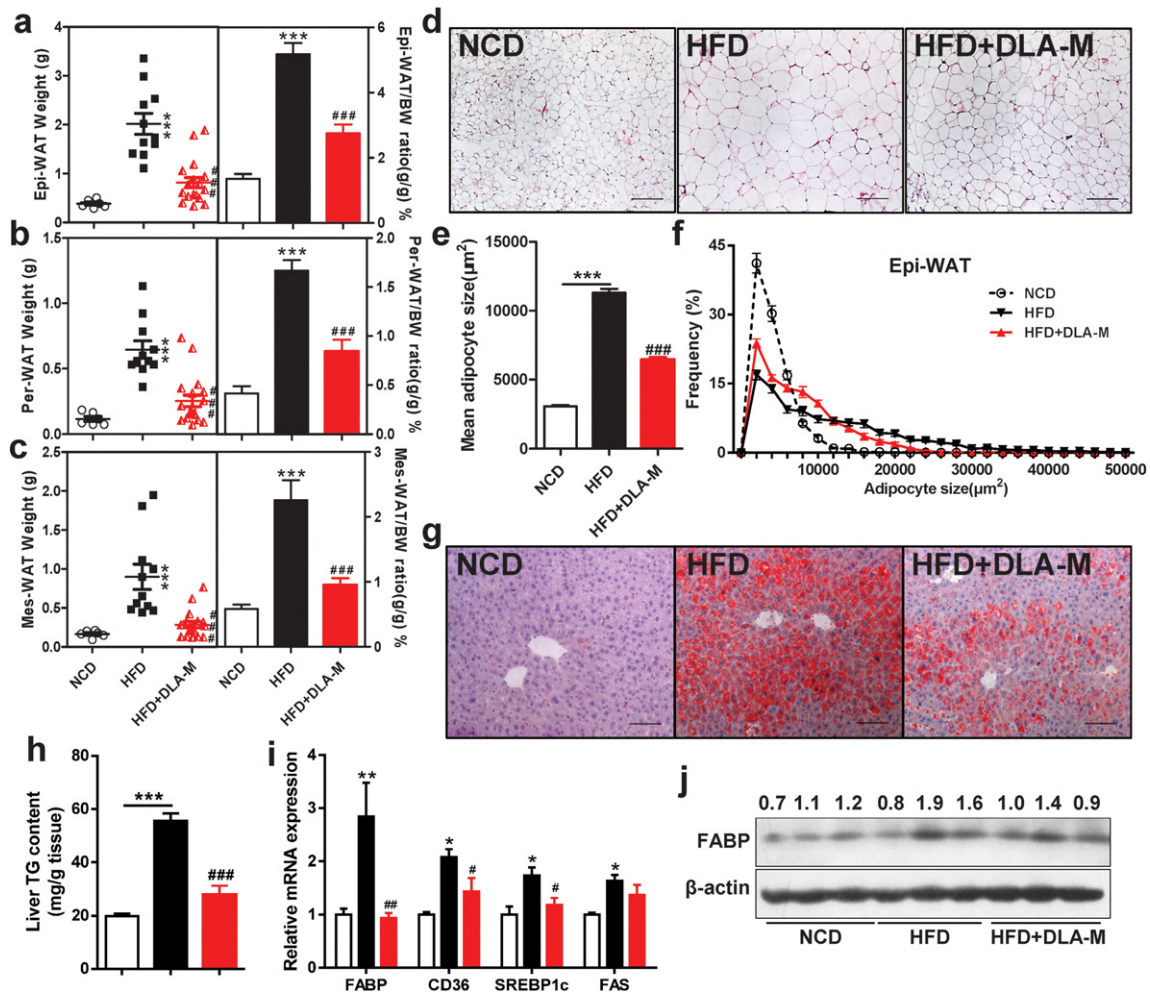
Fig. 2. DLA-M decreases the fat accumulation in the adipose tissues and livers of HFD mice. Epi-WAT weight and Epi-WAT/BW ratio (a), Per-WAT weight and Per-WAT/BW ratio (b), and Mes-WAT weight and Mes-WAT/BW ratio (c) of the mice described in Fig. 1. (d) H&E staining of Epi-WAT sections from mice described in (a) (scale: 200 μm). Mean epididymal adipocyte size (e) and adipocyte size frequency (f) in each group (n = 5 mice per group). (g) Oil Red O staining of liver sections (scale: 100 μm) and liver TG content (h) of mice. (i) Liver mRNA expression of genes involved in lipogenesis was measured by real-time PCR analysis. (j) The FABP protein production (upper panel) and relative protein level (lower panel) were examined in the liver. Values are shown as the means ± s.e.m. *, P < 0.05; **, P < 0.01; ***, and P < 0.001 compared with NCD. #, P < 0.05; ##, P < 0.01; and ###, P < 0.001 compared with HFD by ANOVA with Tukey's multiple comparison test.
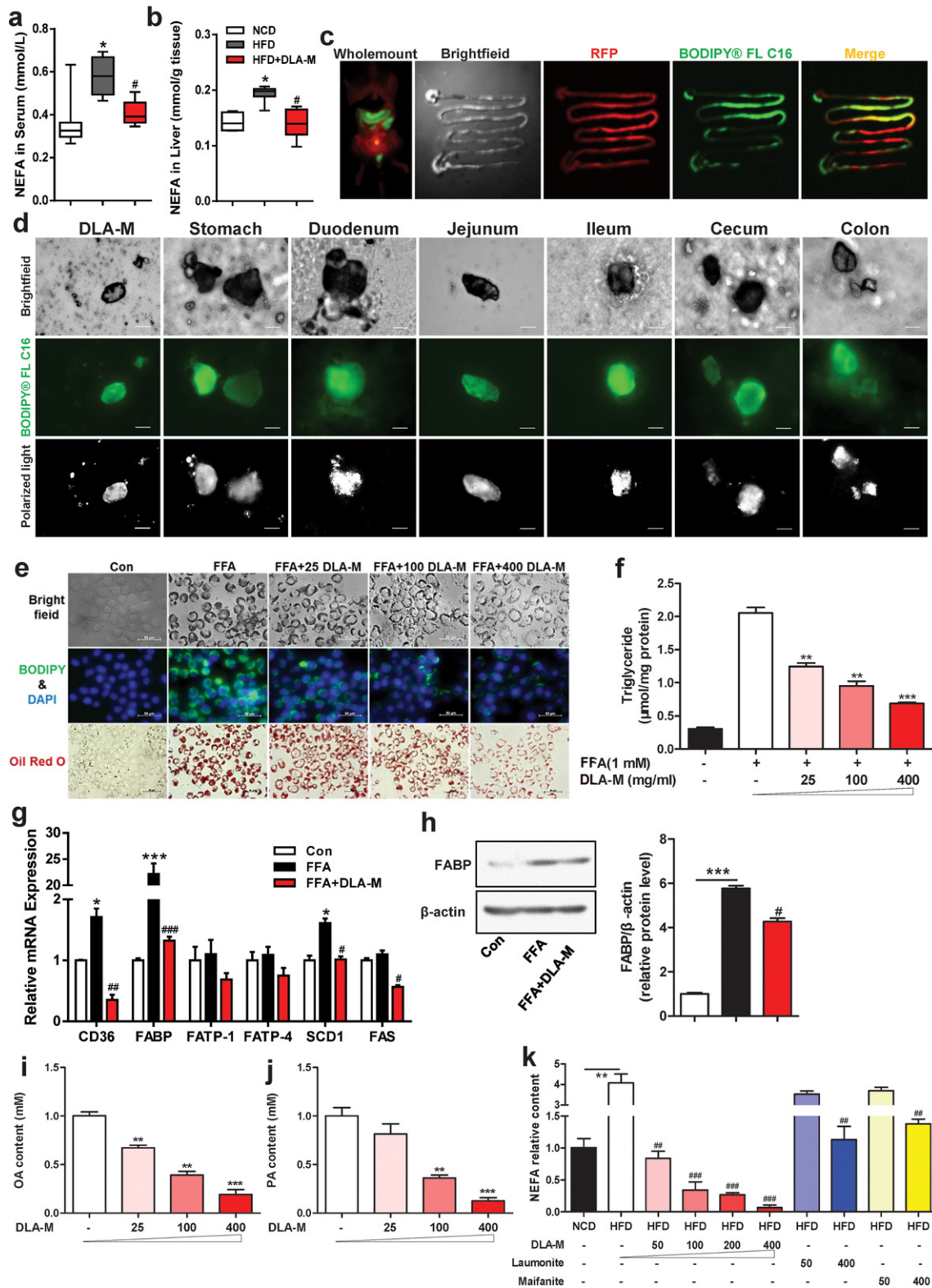
Fig. 3. DLA-M absorbs FFA and prevents hepatic steatosis. Box-plots of the NEFA concentration in the sera (a) and livers (b) of the mice described in Fig. 1. (c) Under a whole-body imaging scope, the RFP mice were separately treated with DLA-M (1 g/kg) and BODIPY® FL C16 (5 mg/kg) by gavage for 4 h. (d) DLA-M absorbs BODIPY® FL C16 *in vitro* (the first panels). Gastrointestinal content smears of mice in (c) in different parts (stomach, duodenum, jejunum, ileum, cecum and colon); in the middle panels, FFA appear green, and the lower panels show polarized light microscopy images of DLA-M crystals (scale: 20 μm). (e) BODIPY and Oil Red O staining of steatotic L-02 cells that were treated with a 1 mM free fatty acid (FFA) mixture (oleic acid and palmitic acid at a molar ratio of 2:1) for 48 h after treatment with 0–400 mg/ml DLA-M using a Transwell model (scale: 50 μm). (f) Quantification of the intracellular triglyceride levels in (e). (g) The mRNA expression levels of fatty acid transport and lipogenic genes were measured by real-time PCR. (h) The FABP protein production was examined by western blotting and the relative protein level was normalized to β-actin. Sodium OA (1 mM) that was dissolved in PBS and PA that was dissolved in methanol (1 mM) were treated with 0–400 mg/ml DLA-M: OA content (i) and PA content (j) in the supernatant. (k) Separated intestinal contents of mice fed a NCD or HFD: saline was added (1:20), and the samples were treated with 0–400 mg/ml DLA-M, laumontite and maifanite for 6 h. Then, the relative content of NEFA was measured. Values are shown as the mean ± s.e.m. *, $P < 0.05$; **, $P < 0.01$; and ***, $P < 0.001$ compared with NCD/Con. #, $P < 0.05$; ##, $P < 0.01$; and ###, $P < 0.001$ compared with HFD/FFA by ANOVA with Tukey's multiple comparison test.

and liver NEFA levels in mice. DLA-M treatment restored the NEFA concentration to near normal levels in HFD-fed mice (Fig. 3a and b). To directly observe the DLA-M adsorption of FFA, mice expressing red fluorescent protein were separately treated with DLA-M and BODIPY® FL C16 (a green fluorescent fatty acids) by gavage. A whole-body imaging scope showed that the entire digestive tract was full of green fluorescent fatty acid (Fig. 3c). Furthermore, we isolated different parts of gastrointestinal tract (stomach, duodenum, jejunum, ileum, cecum and colon) and prepared smears. Combined application of fluorescence and polarized light microscopy showed that DLA-M crystals immobilized green fluorescent fatty acid *in situ* (Fig. 3d). Moreover, we modified a previously described experimental model of hepatocellular steatosis (Gomez-Lechon et al., 2007), and we performed treatment with a gradient concentration of DLA-M by using Transwell equipment. The lipophilic dye Oil Red O and the BODIPY staining and triglyceride content measurements demonstrated that DLA-M significantly decreased the intracellular lipid accumulation in a dose-dependent manner (Fig. 3e and f). In the hepatic cellular model of steatosis, the expression of fatty acid transport (CD36 and FABP) and lipogenic (SCD1 and FAS) genes as well as FABP protein was inhibited in L-02 cells cultured with a FFA mixture after treatment with DLA-M (Fig. 3g and h). We dissolved 1 mM OA and 1 mM PA, and then treated each of the solutions with 0–400 mg/ml DLA-M. As shown in Fig.3i and j, DLA-M also adsorbed OA and PA in a concentration-dependent manner.

To mimic the physiological conditions of the intestinal environment as previously described (Xu et al., 2016), we separated the intestinal chyme from NCD- and HFD-fed mice and mixed the chyme with a suitable amount of saline; then, the mixture was treated with DLA-M and two other aluminosilicate clays (maifanite and laumontite). Afterward, we evaluated the relative NEFA contents in the supernatant. DLA-M exhibited more powerful adsorption ability for NEFA than the other two aluminosilicate clays in this system (Fig. 3k).

3.4. DLA-M Reduces Inflammation via Immobilizing Endotoxin in the Digestive Tract

Obesity and insulin resistance are characterized by low-grade chronic inflammation, whose molecular origin remains unknown (Shi et al., 2006, Cani et al., 2007). Metabolic endotoxemia (the plasma concentration of LPS) initiates the inflammatory tone and obesity-associated insulin resistance (Cani et al., 2008, Chang et al., 2015). We examined the effects of DLA-M on serum endotoxin and inflammation factor (TNFα and IL-6) levels. DLA-M treatment restored the endotoxin, TNFα and IL-6 concentrations to near normal levels in HFD-fed mice, and this change was accompanied by decreased expression of inflammatory factor genes (TNFα, IL-6 and COX-2) in the liver (Fig. 4a–c). Toll-like receptor 4 (TLR-4) signaling pathways are strongly associated with low-grade systemic inflammation and induce the production of
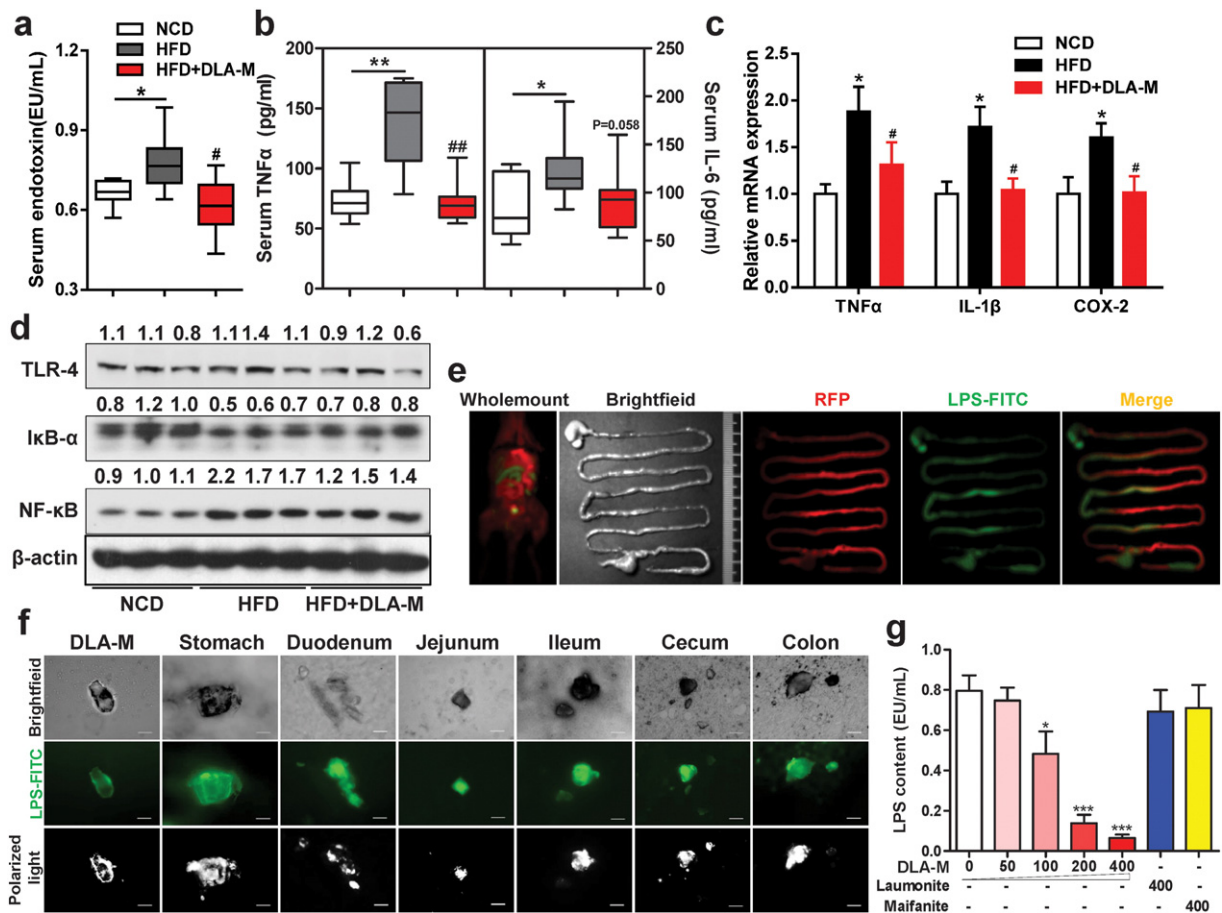
Fig. 4. DLA-M absorbs endotoxin and decreases endotoxemia. Box-plots of the endotoxins (a), TNFα and IL-6 (b) concentrations in the serum of the same mice as in Fig. 1. (c) The liver mRNA expression levels of TNFα, IL-6 and COX-2 were measured by real-time PCR. (d) The liver TLR-4, IκB-α and NF-κB protein production was examined by western blotting and relative protein level was normalized with β-actin. (e) Under a whole-body imaging scope, the RFP mice were separately treated with DLA-M (1 g/kg) and FITC-LPS (5 mg/kg) by gavage for 4 h. (f) DLA-M absorbs FITC-LPS *in vitro* (the first panels). Gastrointestinal content smears of mice in (e) in different tissues (stomach, duodenum, jejunum, ileum, cecum and colon); in the middle panels, LPS appear green, and the lower panels show polarized light microscopy images of DLA-M crystals (scale: 20 μm). LPS (5 mg/ml) dissolved in PBS was treated with 0–400 mg/ml DLA-M, laumontite and maifanite for 6 h: the LPS content (g) in the supernatant was examined. Values are shown as the mean ± s.e.m. *, P < 0.05; **, P < 0.01; and ***, P < 0.001 compared with NCD. #, P < 0.05; and ##, P < 0.01 compared with HFD by ANOVA with Tukey's multiple comparison test.

proinflammatory cytokines by modulating the activity of NF-κB in response to an HFD (Kim et al., 2012, Shi et al., 2006, Cai et al., 2005). We examined whether DLA-M treatment could affect these pathways. As shown in Fig. 4d, compared with the HFD alone, DLA-M supplementation inhibited the TLR-4 and NF-κB protein expression and enhanced the production of IκB-α in the liver. Because DLA-M does not enter the circulatory system, we hypothesized that DLA-M had a fixing effect on the LPS from Gram-negative bacteria in the digestive tract. Thus, using LPS-FITC (LPS labeled with a green fluorescence) as in a previous method, we directly observed DLA-M crystals that immobilized green fluorescent LPS *in situ* in the digestive tract (Fig. 4e and f). Furthermore, we dissolved LPS (200 pg/ml) in PBS and treated samples with 0–400 mg/ml DLA-M, maifanite and laumontite; then, we examined the LPS content in the supernatant. DLA-M showed a dose-dependent adsorption of LPS in this system (Fig. 4g).

3.5. DLA-M Alters Intestinal Morphology of HFD Mice

HFD animals have decreased intestinal permeability, thus leading to the release of LPS from bacteria into the bloodstream (Chang et al., 2015). Compared with HFD controls, the mice that received DLA-M supplementation exhibited a marked increase in the small intestine length at sacrifice, whereas there were no differences in the small intestinal weight (Fig. 5a, b and Supplementary Fig. 3c, d). Otherwise, no significant differences were observed in the lengths and weights of the colon, stomach and cecum (Supplementary Fig. 3a, b and e–j). To further investigate the changes in intestinal morphology, we measured the villus length in the proximal jejunum and found that it was increased in DLA-M-treated mice fed an HFD (Fig. 5c and d). As shown in Fig. 5e, HFD feeding down-regulated the relative mRNA expression of occludin, whereas treatment with DLA-M markedly restored the expression to a near normal level. These results suggested that the oral administration of DLA-M has the potential to inhibit the HFD-induced intestinal inflammation and metabolic endotoxemia induced by HFD and almost completely restores the expression of tight junction proteins.

3.6. DLA-M Modulates the Gut Microbiota Composition of HFD-fed Mice

The gut microbiota of obese humans and HFD-fed mice has been suggested to participate in the pathogenesis of low-grade inflammation and the development of obesity-related metabolic disorders (Zhang et al., 2015). We evaluated the effects of DLA-M on the gut microbiota composition by performing a pyrosequencing-based analysis of the bacterial 16S rRNA V3–V4 region in feces. Using 97% identity as the cutoff, 539 OTUs were delineated. OTU-Venn showed the difference in three groups (Fig. 6a). The Shannon curves and index analysis indicated that the current sequencing depth covered rare new phylotypes and most of the gut microbial diversity, and there were no significant differences in the richness and diversity among the three groups in this study (Supplementary Fig. 4a). UniFrac PCoA revealed a distinct clustering of the gut microbiota composition for each treatment group (Fig. 6b). A Bray-Curtis cluster tree revealed a much greater shift in the microbiota between the NCD and HFD groups, and DLA-M treatment caused a slight reversion of the change that was induced by HFD feeding (Fig. 6c). We observed differences in the OTU abundance at the phylum level. Comparison of the phylum-level proportional abundance and the proportion of OTUs classified at the phylum rank in feces showed that DLA-M treatment had a slight reversion effect of the change that was induced by HFD in Bacteroidetes, Verrucomicrobia and Tenericutes (Fig. 6d and e). However, HFD feeding significantly decreased the ratio of Bacteroidetes to Firmicutes by 54.7% compared with that of NCD mice, whereas there was no difference between HFD and HFD + DLA-M mice (Supplementary Fig. 4b). Comparison of the genus-level proportional abundance showed a clear reversion for the various bacteria (Supplementary Fig. 4c). To identify the specific bacterial phylotypes of microbiota responding to DLA-M treatment, redundancy analysis
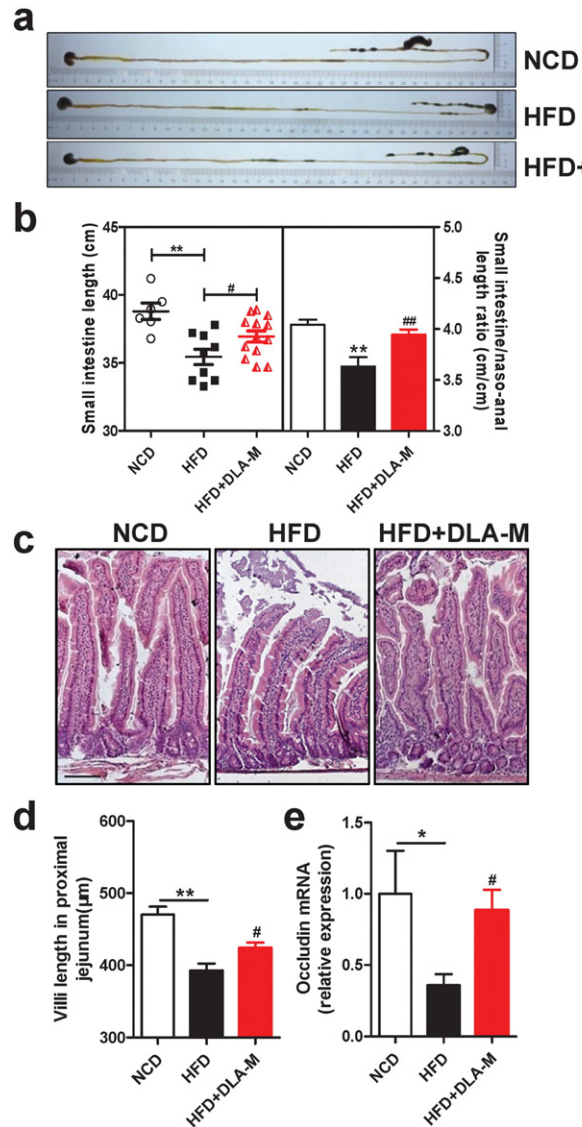
Fig. 5. DLA-M alters the intestinal morphology of HFD-fed mice. (a) Representative images of the gastrointestinal system (stomach, duodenum, jejunum, ileum, cecum and colon). (b) The small intestine length and small intestine/naso-anal length ratio in the mice are notated as in Fig. 1. (c) H&E staining of proximal jejunum sections from mice described in (A) (scale: 100 μm). (d) Proximal jejunum villi length. (e) The intestinal (ileum) mRNA expression of occludin was measured by real-time PCR. Values are shown as the means ± s.e.m. *, $P < 0.05$; **, $P < 0.01$; and ***, $P < 0.001$ compared with NCD. #, $P < 0.05$; and ##, $P < 0.01$ compared with HFD by ANOVA with Tukey's multiple comparison test.

(RDA) was used to analyze the effective sequences of all samples ($P < 0.01$). Compared with the OTUs in NCD mice, 70 OTUs (25 increased and 45 decreased) were significantly altered in HFD mice. Compared with HFD mice, mice that received DLA-M supplementation exhibited changes in 13 OTUs (7 increased and 6 decreased), thus resulting in significant changes in a total of 77 distinct OTUs. Among the 77 OTUs that were altered compared with those in HFD-fed mice, 6 OTUs had changes that were reversed to the direction of those in NCD mice in response to DLA-M treatment (Fig. 6f, g and Supplementary Data 1). Detailed analysis of the 6 OTUs with changes that were reversed by DLA-M supplementation indicated that the changes in *Desulfovibrionaceae* (Sun et al., 2016), *Ruminococcaceae* (Kim et al., 2012), *Bacteroides* (Yan et al., 2013), and *Blautia* (Zhang et al., 2015) were all reversed by DLA-M, and they all positively correlated with obesity in previous studies.

LEfSe results showed the most differently abundant taxons of the three groups (Fig. 7a). The relative abundance of *Blautia* and

Desulfovibrio was also identified by an additional (unpaired) Wilcoxon rank-sum test ($P < 0.05$), and these differences were consistent with the DLA-M-induced reversal (Fig. 7b and c).

Collectively, our data suggested that DLA-M treatment has the potential to improve the gut microbiota dysbiosis induced by an HFD in our model.
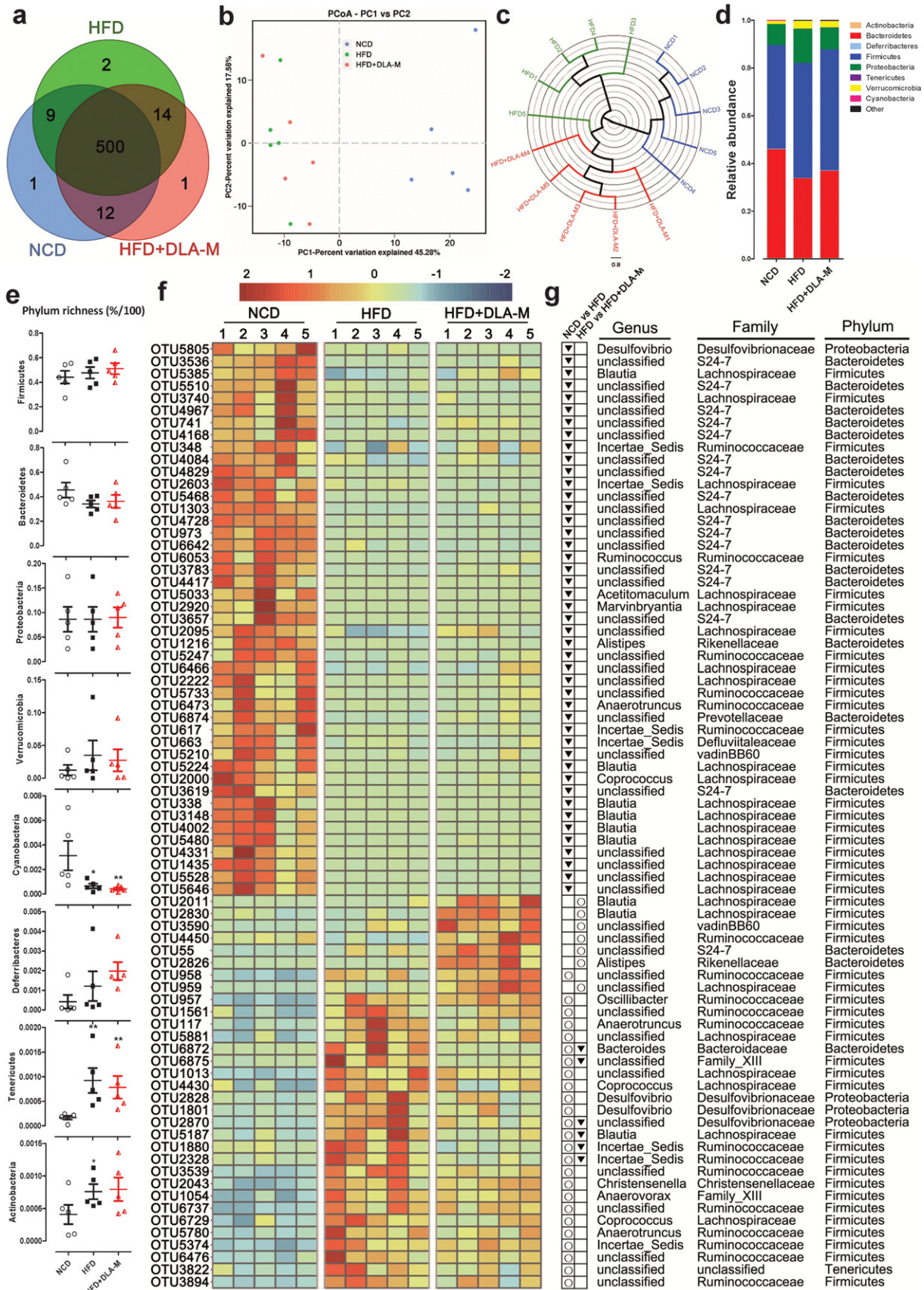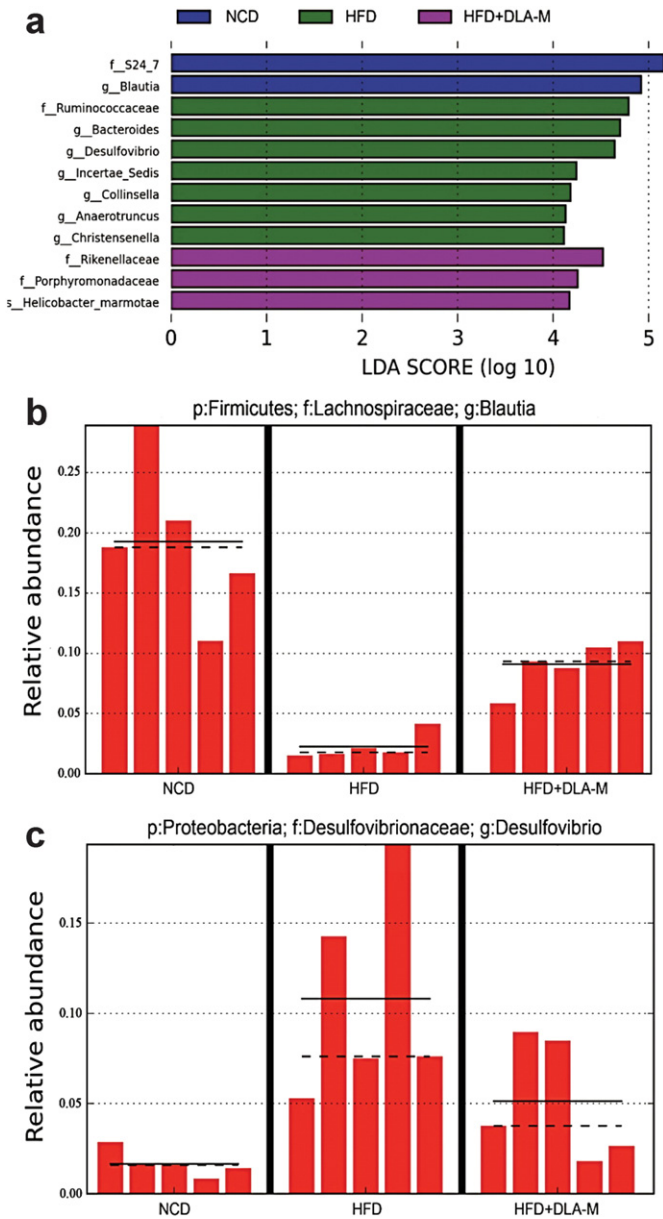
Fig. 7. LEfSe identifies the most differently abundant taxons in the gut microbiota. (a) Only taxa meeting a significant LDA threshold of >4 are shown in the feces of mice as notated in Fig. 1. The relative abundance of *Blautia* (b) and *Desulfovibrio* (c) was obtained from the fecal microbiota from LEfSe results. Solid and dashed lines indicate the mean and median, respectively.

4. Discussion

Montmorillonite, a versatile natural layered aluminosilicate clay mineral, has been found to bind viruses, bacteria and their toxins, suppressing their negative influence on the digestive system. Moreover, montmorillonite can coat the gastrointestinal mucosa and consequently improve the defensive function against aggressive factors (Yen, 2006). Montmorillonite is recommended as an over-the-counter medicine for treating acute and chronic diarrhea and irritable bowel syndrome

(IBS), owing to its strong adsorption (Guarino et al., 2001, Ducrotte et al., 2005). In our previous study, we demonstrated that montmorillonite adsorbs dietary triglycerides and cholesterol and increases fecal lipid excretion, thereby preventing obesity in an HFD-fed rat model (Xu et al., 2016). Lack of physical activity, excess food calorie intake and genetic susceptibility are thought to explain most cases of overweight and obesity at the individual level (Lau et al., 2007). Preventing excessive energy or some obesity-causing harmful metabolites of the gut from reaching the circulatory system is one effective strategy for preventing obesity. Herein, we found further evidence that DLA-M also immobilizes FFA and endotoxin in the digestive system and prevents them from moving into the circulatory system though the adsorption-excretion axis (Supplementary Video 1).

The cross-talk among adipose tissue, insulin resistance, systemic inflammation and intestinal microbiota is of crucial importance for illustrating the underlying mechanisms of obesity-related diseases. Previous studies have indicated that HFD-induced low-grade inflammation, obesity and diabetes can be explained by changes in the gut microbiota and increase the plasma concentration of LPS *i.e.*, induce metabolic endotoxemia (Cani et al., 2008, Chang et al., 2015). The plasma FFA levels are elevated in most obese people after consumption of a fatty meal (Boden et al., 1994). Acute elevation of FFA causes peripheral and hepatic insulin resistance and proinflammatory cytokine release through activation of the NF-κB pathway, thus indicated that FFA is a major link between HFD-induced obesity and the development of systemic inflammation (Itani et al., 2002, Boden et al., 2005). As shown in Figs. 3 and 4, DLA-M treatment significantly decreased the NEFA (−32.5%) and endotoxin (−20.0%) levels in the serum of HFD mice *in vivo*. The NEFA in serum is almost entirely derived from the hydrolysis of TG, which is present at high levels in fatty food and adipose tissue (Karpe et al., 2011), and serum endotoxin is mainly produced by gut microbiota (Cani et al., 2007). We further investigated how DLA-M adsorbs FFA and LPS *in vitro*. DLA-M adsorbs FFA and LPS when changes occur in the surrounding conditions, such as the corresponding solution, cell culture medium and concentration of intestinal chyme. Moreover, using a combination of the fluorescent tracer technique and polarized light microscopy, we observed that DLA-M crystals immobilized BODIPY® FL C16 and FITC-LPS, respectively, in the digestive tract *in situ* (Figs. 3d and 4f). Owing to the adsorption by DLA-M in the gut, lower amounts of FFA and LPS enter the blood circulation system, thereby attenuating hyperlipidemia and endotoxemia; these changes decrease the body weight, inflammation and insulin resistance *in vivo*.

In recent years, an imbalance in the intestinal microbiota composition, also known as gut dysbiosis, has been shown to play an important role in the etiology of obesity and related comorbidities, such as insulin resistance, hyperlipidemia, chronic inflammation, diabetes, NAFLD and atherosclerosis (Lozupone et al., 2012, Tai et al., 2015). Our data show that DLA-M produces mild changes in the composition of the intestinal microbiota, particularly by influencing the bacteria in a manner that is positively correlated with obesity and inflammation. Previous studies have demonstrated that the short-chain fatty acids (SCFAs), which are also referred to as volatile fatty acids (VFAs) and include acetic acid, propionic acid and butyric acid, are produced from the fermentation of polysaccharides and regulate inflammatory responses by suppressing proinflammatory cytokine release (Smith et al., 2013, Maslowski et al., 2009). Recently, Zhang et al. have shown that berberine-mediates the increase in SCFA-producing bacteria. *Blautia* may be involved in relieving inflammation, insulin resistance and obesity in HFD rats (Zhang et al., 2012, 2015). Here, we observed that DLA-M supplementation

Fig. 6. DLA-M alters the gut microbiota composition in HFD mice. (a) OTU-Venn of gut microbiota in the three groups as in Fig. 1. (b) The plots shown were generated using the weighted version of the UniFrac-based PCoA. (c) Bray-Curtis cluster tree using the UPGMA. Comparison of the phylum-level proportional abundance (d), richness represented as the proportions of OTUs classified at the phylum rank (e) (n = 5). *, P < 0.05 and **, P < 0.01 compared with NCD based on the Mann-Whitney test. (f) Heat map showing the relative abundance of RDA-identified key OTUs that were significantly altered by DLA-M in the HFD mice. (g) Representative bacterial taxa information (genus, family and phylum) of 77 OTUs from (f) are shown. White circles and black triangles indicate the OTUs that increased or decreased, respectively, in the NCD and HFD + DLA-M groups relative to the HFD group on the basis of the Turkey (HSD) test (P < 0.05).

reversed the decrease in the relative abundance of *Blautia* caused by HFD administration in mice (Fig. 7b). In addition, we also found a significantly reduction in the relative abundance of endotoxin-producing opportunistic pathogens *Desulfovibrio* (Fig. 7c), a result consistent with findings from previous study in which a prebiotic intervention has been found to decrease the *Desulfovibrio* abundance induced by HFD feeding (Sun et al., 2016, Xiao et al., 2014). Intriguingly, the increase in the Bacteroidetes to Firmicutes ratio has previously been reported to be associated with anti-obesity, but was not observed in the present study (Supplementary Fig. 4b).

In conclusion, our results show that DLA-M immobilizes triglycerides, cholesterol, FFA and endotoxin in the digestive tract *via* the adsorption-excretion axis and thus decrease body weight gain. In addition, the positive influence of DLA-M on HFD-induced gut dysbiosis, especially *Blautia* and *Desulfovibrio*, may partially contribute to the attenuation of intestinal and systemic inflammation and the prevention of obesity-related metabolic disorders.

Supplementary data to this article can be found online at http://dx.doi.org/10.1016/j.ebiom.2017.01.019.

Author Contributions

Y.Z., P.X. and Y.C. contributed to the study concept and design; Y.Z. obtained funding and provided the essential materials; P.X., F.H., J.W., S.D., S.W. and J.L. performed the experiments; P.X., F.H., J.W., X.J. and F.W. analyzed the data; P.X. and Y.Z. wrote the manuscript. All authors reviewed the final manuscript.

Conflicts of Interest

The authors have declared that no competing interests exist.

Acknowledgements/Funding

References

Arner, P., Ryden, M., 2015. Fatty acids, obesity and insulin resistance. Obes. Facts 8, 147–155.
Arnold, M., Pandeya, N., Byrnes, G., Renehan, A.G., Stevens, G.A., Ezzati, M., Ferlay, J., Miranda, J.J., Romieu, I., Dikshit, R., Forman, D., Soerjomataram, I., 2015. Global burden of cancer attributable to high body-mass index in 2012: a population-based study. Lancet Oncol. 16, 36–46.
Bhaskaran, K., Douglas, I., Forbes, H., Dos-Santos-Silva, I., Leon, D.A., Smeeth, L., 2014. Body-mass index and risk of 22 specific cancers: a population-based cohort study of 5.24 million UK adults. Lancet 384, 755–765.
Boden, G., Chen, X.H., Ruiz, J., White, J.V., Rossetti, L., 1994. Mechanisms of fatty acid-induced inhibition of glucose-uptake. J. Clin. Investig. 93, 2438–2446.
Boden, G., She, P., Mozzoli, M., Cheung, P., Gumireddy, K., Reddy, P., Xiang, X., Luo, Z., Ruderman, N., 2005. Free fatty acids produce insulin resistance and activate the pro-inflammatory nuclear factor-kappaB pathway in rat liver. Diabetes 54, 3458–3465.
Bolger, A.M., Lohse, M., Usadel, B., 2014. Trimmomatic: a flexible trimmer for Illumina sequence data. Bioinformatics 30, 2114–2120.
Cai, D.S., Yuan, M.S., Frantz, D.F., Melendez, P.A., Hansen, L., Lee, J., Shoelson, S.E., 2005. Local and systemic insulin resistance resulting from hepatic activation of IKK-beta and NF-kappa B. Nat. Med. 11, 183–190.
Cani, P.D., 2014. Metabolism in 2013 the gut microbiota manages host metabolism. Nat. Rev. Endocrinol. 10, 74–76.
Cani, P.D., Amar, J., Iglesias, M.A., Poggi, M., Knauf, C., Bastelica, D., Neyrinck, A.M., Fava, F., Tuohy, K.M., Chabo, C., Waget, A., Delmee, E., Cousin, B., Sulpice, T., Chamontin, B., Ferrieres, J., Tanti, J.F., Gibson, G.R., Casteilla, L., Delzenne, N.M., Alessi, M.C., Burcelin, R., 2007. Metabolic endotoxemia initiates obesity and insulin resistance. Diabetes 56, 1761–1772.
Cani, P.D., Bibiloni, R., Knauf, C., Neyrinck, A.M., Neyrinck, A.M., Delzenne, N.M., Burcelin, R., 2008. Changes in gut microbiota control metabolic endotoxemia-induced inflammation in high-fat diet-induced obesity and diabetes in mice. Diabetes 57, 1470–1481.
Cani, P.D., Possemiers, S., Van De Wiele, T., Guiot, Y., Everard, A., Rottier, O., Geurts, L., Naslain, D., Neyrinck, A., Lambert, D.M., Muccioli, G.G., Delzenne, N.M., 2009. Changes

in gut microbiota control inflammation in obese mice through a mechanism involving GLP-2-driven improvement of gut permeability. Gut 58, 1091–1103.
Caporaso, J.G., Kuczynski, J., Stombaugh, J., Bittinger, K., Bushman, F.D., Costello, E.K., Fierer, N., Pena, A.G., Goodrich, J.K., Gordon, J.I., Huttley, G.A., Kelley, S.T., Knights, D., Koenig, J.E., Ley, R.E., Lozupone, C.A., Mcdonald, D., Muegge, B.D., Pirrung, M., Reeder, J., Sevinsky, J.R., Tumbaugh, P.J., Walters, W.A., Widmann, J., Yatsunenko, T., Zaneveld, J., Knight, R., 2010. QIIME allows analysis of high-throughput community sequencing data. Nat. Methods 7, 335–336.
Chang, C.J., Lin, C.S., LU, C.C., Martel, J., Ko, Y.F., Ojcius, D.M., Tseng, S.F., Wu, T.R., Chen, Y.Y.M., Young, J.D., Lai, H.C., 2015. *Ganoderma lucidum* reduces obesity in mice by modulating the composition of the gut microbiota. Nat. Commun. 6.
Chen, X., Zhang, C., Zhao, M., Shi, C.E., Zhu, R.M., Wang, H., Zhao, H., Wei, W., LI, J.B., XU, D.X., 2011. Melatonin alleviates lipopolysaccharide-induced hepatic SREBP-1c activation and lipid accumulation in mice. J. Pineal Res. 51, 416–425.
Ducrotte, P., Dapoigny, M., Bonaz, B., Siproudhis, L., 2005. Symptomatic efficacy of beidellitic montmorillonite in irritable bowel syndrome: a randomized, controlled trial. Aliment. Pharmacol. Ther. 21, 435–444.
Edgar, R.C., 2010. Search and clustering orders of magnitude faster than BLAST. Bioinformatics 26, 2460–2461.
Edgar, R.C., Haas, B.J., Clemente, J.C., Quince, C., Knight, R., 2011. UCHIME improves sensitivity and speed of chimera detection. Bioinformatics 27, 2194–2200.
Everard, A., Cani, P.D., 2013. Diabetes, obesity and gut microbiota. Best Pract. Res. Clin. Gastroenterol. 27, 73–83.
Gao, J., He, J., Zhai, Y., Wada, T., Xie, W., 2009. The constitutive androstane receptor is an anti-obesity nuclear receptor that improves insulin sensitivity. J. Biol. Chem. 284, 25984–25992.
Gomez-Lechon, M.J., Donato, M.T., Martinez-Romero, A., Jimenez, N., Castell, J.V., O'connor, J.E., 2007. A human hepatocellular in vitro model to investigate steatosis. Chem. Biol. Interact. 165, 106–116.
Guarino, A., Bisceglia, M., Castellucci, G., Iacono, G., Casali, L.G., Bruzzese, E., Musetta, A., Greco, L., Dia, S.S.G.S.A., 2001. Smectite in the treatment of acute diarrhea: a nationwide randomized controlled study of the Italian Society of Pediatric Gastroenterology and Hepatology (SIGEP) in collaboration with primary care pediatricians. J. Pediatr. Gastroenterol. Nutr. 32, 71–75.
Harte, A.L., Da Silva, N.F., Creely, S.J., Mcgee, K.C., Billyard, T., Youssef-Elabd, E.M., Tripathi, G., Ashour, E., Abdalla, M.S., Sharada, H.M., Amin, A.I., Burt, A.D., Kumar, S., Day, C.P., Mcternan, P.G., 2010. Elevated endotoxin levels in non-alcoholic fatty liver disease. J. Inflamm. London 7.
Hildebrandt, M.A., Hoffmann, C., Sherrill-Mix, S.A., Keilbaugh, S.A., Hamady, M., Chen, Y.Y., Knight, R., Ahima, R.S., Bushman, F., Wu, G.D., 2009. High-fat diet determines the composition of the murine gut microbiome independently of obesity. Gastroenterology 137, 1716–1724.
Hoffmann, L.S., Etzrodt, J., Willkomm, L., Sanyal, A., Scheja, L., Fischer, A.W.C., Stasch, J.P., Bloch, W., Friebe, A., Heeren, J., Pfeifer, A., 2015. Stimulation of soluble guanylyl cyclase protects against obesity by recruiting brown adipose tissue. Nat. Commun. 6, 7235.
Itani, S.I., Ruderman, N.B., Schmieder, F., Boden, G., 2002. Lipid-induced insulin resistance in human muscle is associated with changes in diacylglycerol, protein kinase C, and IkappaB-alpha. Diabetes 51, 2005–2011.
Karpe, F., Dickmann, J.R., Frayn, K.N., 2011. Fatty acids, obesity, and insulin resistance: time for a reevaluation. Diabetes 60, 2441–2449.
Kim, K.A., Gu, W., Lee, I.A., Joh, E.H., Kim, D.H., 2012. High fat diet-induced gut microbiota exacerbates inflammation and obesity in mice via the TLR4 signaling pathway. PLoS One 7.
Lau, D.C.W., Douketis, J.D., Morrison, K.M., Hramiak, I.M., Sharma, A.M., Ur, E., 2007. 2006 Canadian clinical practice guidelines on the management and prevention of obesity in adults and children [summary]. Can. Med. Assoc. J. 176, S1–S13.
Lozupone, C.A., Stombaugh, J.I., Gordon, J.I., Jansson, J.K., Knight, R., 2012. Diversity, stability and resilience of the human gut microbiota. Nature 489, 220–230.
Magoc, T., Salzberg, S.L., 2011. FLASH: fast length adjustment of short reads to improve genome assemblies. Bioinformatics 27, 2957–2963.
Maslowski, K.M., Vieira, A.T., Ng, A., Kranich, J., Sierro, F., Yu, D., Schilter, H.C., Rolph, M.S., Mackay, F., Artis, D., Xavier, R.J., Teixeira, M.M., Mackay, C.R., 2009. Regulation of inflammatory responses by gut microbiota and chemoattractant receptor GPR43. Nature 461, 1282–1286.
Musso, G., Gambino, R., Cassader, M., 2010. Obesity, diabetes, and gut microbiota the hygiene hypothesis expanded? Diabetes Care 33, 2277–2284.
Qin, J.J., Li, R.Q., Raes, J., Arumugam, M., Burgdorf, K.S., Manichanh, C., Nielsen, T., Pons, N., Levenez, F., Yamada, T., Mende, D.R., Li, J.H., Xu, J.M., Li, S.C., Li, D.F., Cao, J.J., Wang, B., Liang, H.Q., Zheng, H.S., Xie, Y.L., Tap, J., Lepage, P., Bertalan, M., Batto, J.M., Hansen, T., Le Paslier, D., Linneberg, A., Nielsen, H.B., Pelletier, E., Renault, P., Sicheritz-Ponten, T., Turner, K., Zhu, H.M., Yu, C., Li, S.T., Jian, M., Zhou, Y., LI, Y.R., Zhang, X.Q., Li, S.G., Qin, N., Yang, H.M., Wang, J., Brunak, S., Dore, J., Guarner, F., Kristiansen, K., Pedersen, O., Parkhill, J., Weissenbach, J., Bork, P., Ehrlich, S.D., Wang, J., Consortium, M., 2010. A human gut microbial gene catalogue established by metagenomic sequencing. Nature 464, 59–70.
Segata, N., Izard, J., Waldron, L., Gevers, D., Miropolsky, L., Garrett, W.S., Huttenhower, C., 2011. Metagenomic biomarker discovery and explanation. Genome Biol. 12.
Serino, M., Luche, E., Gres, S., Baylac, A., Berge, M., Cenac, C., Waget, A., Klopp, P., Iacovoni, J., Klopp, C., Mariette, J., Bouchez, O., Lluch, J., Ouarne, F., Monsan, P., Valet, P., Roques, C., Amar, J., Bouloumie, A., Theodorou, V., Burcelin, R., 2012. Metabolic adaptation to a high-fat diet is associated with a change in the gut microbiota. Gut 61, 543–553.
Shen, J., Obin, M.S., Zhao, L.P., 2013. The gut microbiota, obesity and insulin resistance. Mol. Asp. Med. 34, 39–58.
Shi, H., Kokoeva, M.V., Inouye, K., Tzameli, I., Yin, H., Flier, J.S., 2006. TLR4 links innate immunity and fatty acid-induced insulin resistance. J. Clin. Investig. 116, 3015–3025.

Shin, N.R., Lee, J.C., Lee, H.Y., Kim, M.S., Whon, T.W., Lee, M.S., Bae, J.W., 2014. An increase in the *Akkermansia* spp. population induced by metformin treatment improves glucose homeostasis in diet-induced obese mice. Gut 63, 727–735.

Smith, P.M., Howitt, M.R., Panikov, N., Michaud, M., Gallini, C.A., Bohlooly, Y.M., Glickman, J.N., Garrett, W.S., 2013. The microbial metabolites, short-chain fatty acids, regulate colonic Treg cell homeostasis. Science 341, 569–573.

Sun, J., Ren, F.Z., Xiong, L., Zhao, L., Guo, H.Y., 2016. Bovine lactoferrin suppresses high-fat diet induced obesity and modulates gut microbiota in C57BL/6J mice. J. Funct. Foods 22, 189–200.

Tai, N., Wong, F.S., Wen, L., 2015. The role of gut microbiota in the development of type 1, type 2 diabetes mellitus and obesity. Rev. Endocr. Metab. Disord. 16, 55–65.

Thuy, S., Ladurner, R., Volynets, V., Wagner, S., Strahl, S., Konigsrainer, A., Maier, K.P., Bischoff, S.C., Bergheim, I., 2008. Nonalcoholic fatty liver disease in humans is associated with increased plasma endotoxin and plasminogen activator inhibitor 1 concentrations and with fructose intake. J. Nutr. 138, 1452–1455.

Wormser, D., Kaptoge, S., Di Angelantonio, E., Wood, A.M., Pennells, L., Thompson, A., Sarwar, N., Kizer, J.R., Lawlor, D.A., Nordestgaard, B.G., Ridker, P., Salomaa, V., Stevens, J., Woodward, M., Sattar, N., Collins, R., Thompson, S.G., Whitlock, G., Danesh, J., Factors, E.R., 2011. Separate and combined associations of body-mass index and abdominal adiposity with cardiovascular disease: collaborative analysis of 58 prospective studies. Lancet 377, 1085–1095.

Xiao, S., Fei, N., Pang, X., Shen, J., Wang, L., Zhang, B., Zhang, M., Zhang, X., Zhang, C., Li, M., Sun, L., Xue, Z., Wang, J., Feng, J., Yan, F., Zhao, N., Liu, J., Long, W., Zhao, L., 2014. A gut microbiota-targeted dietary intervention for amelioration of chronic inflammation underlying metabolic syndrome. FEMS Microbiol. Ecol. 87, 357–367.

Xu, P.F., Dai, S., Wang, J., Zhang, J., Liu, J., Wang, F., Zhai, Y.G., 2016. Preventive obesity agent montmorillonite adsorbs dietary lipids and enhances lipid excretion from the digestive tract. Sci. Rep. 6.

Yan, H., Potu, R., Lu, H., De Almeida, V.V., Stewart, T., Ragland, D., Armstrong, A., Adeola, O., Nakatsu, C.H., Ajuwon, K.M., 2013. Dietary fat content and fiber type modulate hind gut microbial community and metabolic markers in the pig. PLoS One 8.

Yen, Z.S., 2006. Smectite for acute diarrhoea in children. Emerg. Med. J. 23, 65–66.

Zhang, X., Zhao, Y., Zhang, M., Pang, X., Xu, J., Kang, C., Li, M., Zhang, C., Zhang, Z., Zhang, Y., Li, X., Ning, G., Zhao, L., 2012. Structural changes of gut microbiota during berberine-mediated prevention of obesity and insulin resistance in high-fat diet-fed rats. PLoS One 7, e42529.

Zhang, X., Zhao, Y.F., Xu, J., Xue, Z.S., Zhang, M.H., Pang, X.Y., Zhang, X.J., Zhao, L.P., 2015. Modulation of gut microbiota by berberine and metformin during the treatment of high-fat diet-induced obesity in rats. Sci. Rep. 5.

Zhou, S.W., Zhang, M., Zhu, M., 2014. Liraglutide reduces lipid accumulation in steatotic L-02 cells by enhancing autophagy. Mol. Med. Rep. 10, 2351–2357.